Liquid Crystals
Publication details, including instructions for authors and subscription information:
http://www.informaworld.com/smpp/title~content=t713926090

Anchoring transition of bent-rod liquid crystal dimers on different surfaces

Guksik Lee[a]; Hyeon-cheol Jeong[ab]; Fumito Araoka[a]; Ken Ishikawa[a]; Jong Gun Lee[b]; Kyung-Tae Kang[b]; Mojca Cepic[c]; Hideo Takezoe[a]
[a] Department of Organic and Polymeric Materials, Tokyo Institute of Technology, Tokyo, Japan [b] Department of Chemistry and Chemistry Institute for Functional Materials, Pusan National University, Pusan, Korea [c] Jozef Stefan Institute, Ljubljana, Slovenia

Online publication date: 06 July 2010

To cite this Article Lee, Guksik , Jeong, Hyeon-cheol , Araoka, Fumito , Ishikawa, Ken , Gun Lee, Jong , Kang, Kyung-Tae , Cepic, Mojca and Takezoe, Hideo(2010) 'Anchoring transition of bent-rod liquid crystal dimers on different surfaces', Liquid Crystals, 37: 6, 883 — 892
To link to this Article: DOI: 10.1080/02678292.2010.481904
URL: http://dx.doi.org/10.1080/02678292.2010.481904

Liquid Crystals,
Vol. 37, Nos. 6–7, June–July 2010, 883–892

Taylor & Francis
Taylor & Francis Group

INVITED ARTICLE

Anchoring transition of bent-rod liquid crystal dimers on different surfaces

Guksik Lee[a], Hyeon-cheol Jeong[a,b], Fumito Araoka[a], Ken Ishikawa[a], Jong Gun Lee[b], Kyung-Tae Kang[b], Mojca Cepic[c] and Hideo Takezoe[a]*

[a]*Department of Organic and Polymeric Materials, Tokyo Institute of Technology, 2–12–1, O-okayama, Meguro–ku, Tokyo 152–8552, Japan;* [b]*Department of Chemistry and Chemistry Institute for Functional Materials, Pusan National University, San 30, Jangjeon–dong, Guemjeong–gu, Pusan 609–735, Korea;* [c]*Jozef Stefan Institute, Jamova 39, 1000 Ljubljana, Slovenia*

(*Received 9 December 2009; accepted 16 March 2010*)

Non-symmetrical dimers have been synthesised, in which bent- and rod-shaped mesogenic molecules are linked by a flexible polymethylene spacer $-(CH_2)_n-$. It has been shown that compounds in which $n = 5$, 6 or 7 exhibit one (nematic), two (nematic and smectic), and no mesogenic phases, respectively. These exhibit a variety of anchoring transition behaviours depending on the mesogenic molecules ($n = 5$ or 6) and surfaces (polyimide surfaces for homeotropic and planar alignment, or a perfluoropolymer surface). Discontinuous and continuous planar-to-homeotropic orientational changes take place with decreasing temperature. These differences may originate from different dielectric anisotropy, and steric interactions caused by the directional relationship of bent and rod mesogens, depending on the length of the spacer. A possible explanation is suggested on the basis of surface–molecule interactions.

Keywords: bent-rod liquid crystal dimer; anchoring transition; surface interaction; dielectric anisotropy; polyimide; perfluoropolymer; phenomenological theory

1. Introduction

Since liquid crystals are fluid, containers such as a pair of glass substrates are required if they are to be used in devices. To produce appropriate orientations for particular uses such as displays, surfaces usually have to be treated. Interactions between surfaces and liquid crystal molecules are therefore an important issue from the applicational viewpoint. Since liquid crystals are anisotropic, a variety of anisotropic surface interactions emerge. This also makes such surface interactions very important from a scientific viewpoint.

An important example related to surface interactions is the biaxial nematic (N_B) phase. The N_B phase was first confirmed experimentally to exist in a lyotropic ternary system by Yu and Saupe [1]. Critical behaviour of biaxial–uniaxial nematic (N_B–N_U) phase transitions in amphiphilic systems has also been discussed by Boonbrahm and Saupe [2]. Recently, Le *et al.* [3] have claimed that the existence of the N_B phase and the N_B–N_U transition reported by Prasad *et al.* [4] was erroneous, and suggested that an anchoring transition may appear to be the N_B–N_U phase transition.

In addition, Dhara *et al.* [5] have reported that a perfluoropolymer provides an interesting surface on which some liquid crystals exhibit orientational change, or anchoring transition, with temperature variation. Moreover, the transition from planar-to-homeotropic or homeotropic-to-planar is first order (discontinuous) or second order (continuous), and is associated with large or small orientational changes depending on the two liquid crystals involved.

Although many experimental and theoretical studies have been made [6–10], further systematic studies are still required to understand fully the anchoring transition phenomenon. In the present work, bent-rod liquid crystal dimers have been synthesised to observe the anchoring transition. Since the dimer consists of bent-core and cyanobiphenyl mesogenic groups linearly linked by a polymethylene spacer which have transverse and longitudinal dipoles, respectively, it has been possible to examine the effect of large dipoles on the anchoring transition. The anchoring transitional behaviour of these homologues has been studied on three different surfaces.

2. Experimental

2.1 Synthesis

A novel homologous series of bent-rod dimers B*n*R (Scheme 1, $n = 5$–7) has been synthesised, consisting of bent-core and rod-shaped mesogens. These are conventional disubstituted isophthalate derivatives (bent-core liquid crystals) with a rod-like cyanobiphenyl monosubstituted on to a bent mesogen unit through a flexible polymethylene spacer $-(CH_2)_n-$.

*Corresponding author. Email: takezoe.h.aa@m.titech.ac.jp

ISSN 0267-8292 print/ISSN 1366-5855 online

DOI: 10.1080/02678292.2010.481904
http://www.informaworld.com

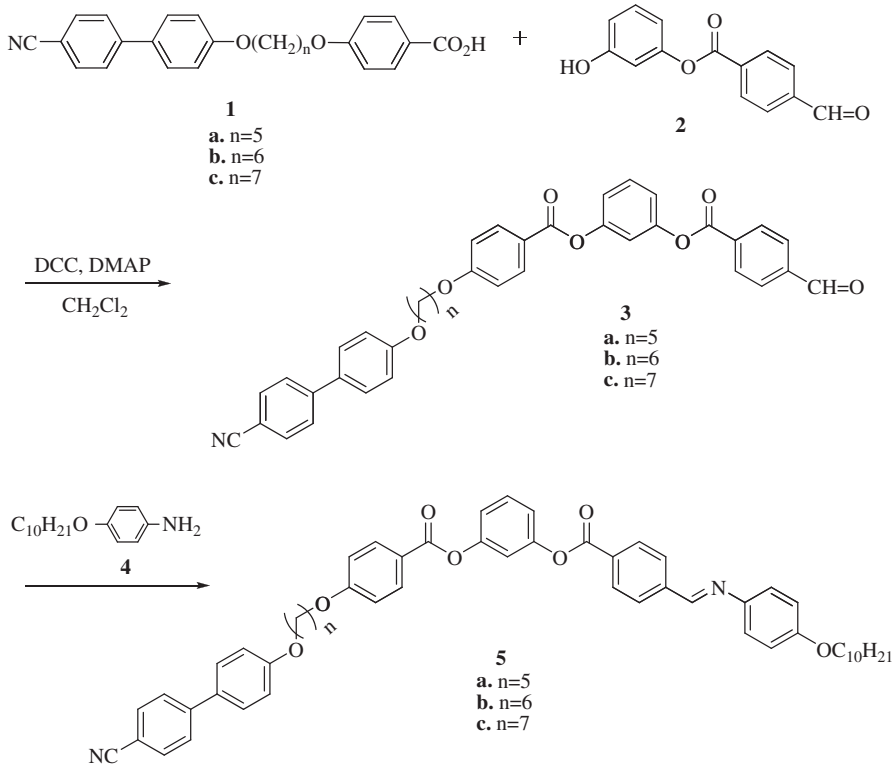

Scheme 1. Synthesis and chemical structure of the bent-core liquid crystal dimers B*n*R.

*2.1.1 Preparation of 3-{4-[5-(4′-cyanobiphenyloxy) alkyloxy]benzoyloxy}phenyl 4-formylbenzoate (**3**)*

A typical procedure for the synthesis of **3a** is as follows. To a solution of N,N-dicyclohexylcarbodiimide (DCC; 0.234 g, 1.13 mmol) in dichloromethane (5 ml) and 4-dimethylaminopyridine (DMAP, 21 mg, 0.18 mmol) were added 4-[5-(4-cyanobiphenyloxy)pentyloxy]-benzoic acid (**1a**) (0.35 g, 0.87 mmol) and 3-hydroxyphenyl-4-formylbenzoate (**2;** 0.21 g, 0.87 mmol). The reaction mixture was heated under reflux for one day. The precipitate was removed by filtration and washed with dichloromethane. The filtrate was washed with aqueous $NaHCO_3$ solution, dried over Na_2SO_4 and concentrated. The residue was purified by column chromatography (silica gel : dichloromethane 1 : 1, $R_f = 0.43$) to give **3a** (0.36 g, 72%). Compounds **3b** and **3c** were prepared similarly, each in 68% yield.

3a: ^{1}H–NMR δ 1.45–1.60 (m, 2H), 1.74–1.98 (m, 4H), 3.99–4.07 (m, 4H), 6.95–7.00 (m, 4H), 7.17 (d, 2H, $J = 8.4$ Hz), 7.45–7.53 (m, 4H), 7.63 (d, 2H, $J = 8.4$ Hz), 7.69 (d, 2H, $J = 8.4$ Hz), 8.02 (d, 2H, $J = 8.7$ Hz), 8.14 (d, 2H, $J = 8.7$ Hz), 8.36 (d, 2H, $J = 8.4$ Hz), 10.01 (s, 1H)

3b: ^{1}H–NMR δ 1.45–1.60 (m, 4H), 1.74–1.98 (m, 4H), 3.99–4.07 (m, 4H), 6.95–7.00 (m, 4H), 7.17 (d, 2H, $J = 8.4$ Hz), 7.45–7.53 (m, 4H), 7.63 (d, 2H, $J = 8.4$ Hz), 7.69 (d, 2H, $J = 8.4$ Hz), 8.02 (d, 2H, $J = 8.7$ Hz), 8.14 (d, 2H, $J = 8.7$ Hz), 8.36 (d, 2H, $J = 8.4$ Hz), 10.01 (s, 1H)

3c: ^{1}H–NMR δ 1.30–1.60 (m, 6H), 1.74–1.98 (m, 4H), 3.99–4.07 (m, 4H), 6.95–7.00 (m, 4H), 7.17 (d, 2H, $J = 8.4$ Hz), 7.45–7.53 (m, 4H), 7.63 (d, 2H, $J = 8.4$ Hz), 7.69 (d, 2H, $J = 8.4$ Hz), 8.02 (d, 2H, $J = 8.7$ Hz), 8.14 (d, 2H, $J = 8.7$ Hz), 8.36 (d, 2H, $J = 8.4$ Hz), 10.01 (s, 1H)

*2.1.2 Preparation of bent-rod dimers (**5**)*

To a solution of **3a** (0.35 g, 0.55 mmol) and 4-decyloxyaniline (**4;** 0.16 g, 0.66 mmol) in chloroform (5 ml) were added molecular sieves (0.25 g) and stirred at room temperature for two days. The reaction mixture was filtered and the filtrate added to cold ethanol to give **5a** (0.32 g, 67%). Compounds **5b** and **5c** were prepared similarly in 70% and 68% yield, respectively.

5a: ^{1}H–NMR δ 0.89 (t, 3H, $J = 6.6$ Hz), 1.30–1.60 (m, 16H), 1.74–1.98 (m, 6H), 3.99–4.07 (m, 6H),

6.93–7.00 (m, 6H), 7.14–7.30 (m, 4H), 7.48–7.53 (m, 4H), 7.63 (d, 2H, $J = 8.4$ Hz), 7.69 (d, 2H, $J = 8.4$ Hz), 8.02 (d, 2H, $J = 7.2$ Hz), 8.13 (d, 2H, $J = 8.4$ Hz), 8.29 (d, 2H, $J = 8.4$ Hz), 8.57 (s, 1H);
^{13}C–NMR δ 14.1, 22.7, 22.8, 26.0, 28.8, 29.0, 29.1, 29.3, 29.4, 29.6, 31.9, 67.9, 68.1, 68.5, 110.2, 110.7, 113.2, 114.4, 114.5, 115.2, 117.0, 119.0, 119.1, 121.7, 121.8, 127.7, 129.1, 129.5, 129.7, 130.4, 130.9, 132.5, 132.7, 141.6, 143.6, 145.1, 151.7, 155.2, 155.6, 159.7, 164.0, 164.2, 164.3, 164.4.

5b: ^{1}H–NMR δ 0.89 (t, 3H, $J = 6.6$ Hz), 1.30–1.60 (m, 18H), 1.74–1.98 (m, 6H), 3.99–4.07 (m, 6H), 6.93–7.00 (m, 6H), 7.14–7.30 (m, 4H), 7.48–7.53 (m, 4H), 7.63 (d, 2H, $J = 8.4$ Hz), 7.69 (d, 2H, $J = 8.4$ Hz), 8.02 (d, 2H, $J = 7.2$ Hz), 8.13 (d, 2H, $J = 8.4$ Hz), 8.29 (d, 2H, $J = 8.4$ Hz), 8.57 (s, 1H);
^{13}C–NMR δ 14.1, 22.7, 22.8, 26.0, 28.8, 29.0, 29.1, 29.2, 29.3, 29.4, 29.6, 31.9, 68.0, 68.2, 68.5, 110.2, 110.7, 113.2, 114.4, 114.5, 115.2, 117.0, 119.0, 119.1, 121.7, 121.8, 127.7, 129.1, 129.5, 129.7, 130.4, 130.9, 132.5, 132.7, 141.6, 143.6, 145.1, 151.7, 155.2, 155.6, 159.7, 164.0, 164.2, 164.3, 164.4.

5c: ^{1}H–NMR δ 0.89 (t, 3H, $J = 6.6$ Hz), 1.30–1.60 (m, 20H), 1.74–1.98 (m, 6H), 3.99–4.07 (m, 6H), 6.93–7.00 (m, 6H), 7.14–7.30 (m, 4H), 7.48–7.53 (m, 4H), 7.63 (d, 2H, $J = 8.4$ Hz), 7.69 (d, 2H, $J = 8.4$ Hz), 8.02 (d, 2H, $J = 7.2$ Hz), 8.13 (d, 2H, $J = 8.4$ Hz), 8.29 (d, 2H, $J = 8.4$ Hz), 8.57 (s, 1H);
^{13}C–NMR δ 14.1, 22.7, 22.8, 25.9, 26.0, 28.8, 29.0, 29.1, 29.2, 29.3, 29.4, 29.6, 31.9, 68.0, 68.2, 68.5, 110.2, 110.7, 113.2, 114.4, 114.5, 115.2, 117.0, 119.0, 119.1, 121.7, 121.8, 127.7, 129.1, 129.5, 129.7, 130.4, 130.9, 132.5, 132.7, 141.6, 143.6, 145.1, 151.7, 155.2, 155.6, 159.7, 164.0, 164.2, 164.3, 164.4.

2.2 *Sample preparation and measurements*

The phase transition temperatures and their associated enthalpies were obtained by differential scanning calorimetry (DSC; Perkin–Elmer, Diamond DSC); they are listed in Table 1.

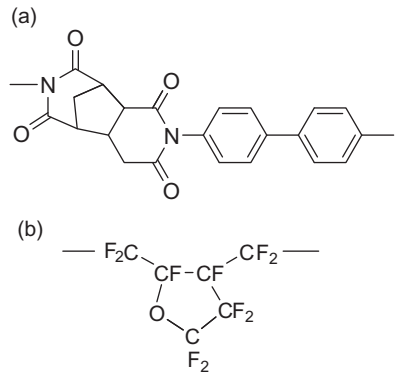

Figure 1. Chemical structure of the polymers used (a) AL1254 and (b) CYTOP.

The smectic A (SmA) phase observed in B6R was found to have a two-molecular layer periodicity by small-angle X-ray diffraction. The detail will be reported separately. Liquid crystal materials were introduced into the cells by means of capillary action in the isotropic phase. The substrate surfaces, with indium tin oxide (ITO), were coated with three different surface agents: polyimide for planar alignment (AL1254, JSR), polyimide for vertical alignment (JALS–204, JSR), and poly[perfluoro(4-vinyloxy-1-butene)] (CYTOP, Asahi Glass). The chemical structures of AL1254 and CYTOP are shown in Figure 1. The chemical structure of JALS–204 has not been disclosed, but it is understood to be a polyamic acid with alkyl side-chains. Alignment layers were rubbed antiparallel to one another. The cell thickness was about 5μm.

The anchoring transition was observed using a polarising optical microscope (Nikon, Optiphot–POL). The temperature was controlled using a hot stage (Mettler, FP82) and controller (Mettler, FP90) to within ± 0.1°C. The birefringence was measured by a Berek compensator (Nichika, No 10547). Dielectric studies were carried out in the frequency range 40 Hz to 100 MHz using an impedance analyser (Agilent, model 4294A).

Table 1. Phase transition temperature (°C) and enthalpies (J g^{-1}) of the compounds B*n*R.

n		Transition temperature (enthalpy)
5	heating	$Cr_1^{(1)}$ 93.6 (6.1) $Cr_2^{(2)}$ 101.0 (13.9) $N^{(3)}$ 122.7 (0.6) $I^{(4)}$
	cooling	Cr_1 76.5 (7.8) Cr_2 88.7 (25.7) N 120.3 (0.6) I
6	heating	Cr 77.6 (17.7) $SmA^{(5)}$ 107.2 (4.7) N 154.2 (1.1) I
	cooling	Cr 56.5 (13.0) SmA 97.9 (1.9) N 154.5 (0.5) I
7	heating	Cr 125.0 (36.6) I
	cooling	Cr 108.8 (56.4) I

Notes: The cell thickness was about 5μ (1), (2): crystalline phase, (3): nematic phase, (4): isotropic liquid, (5): smectic A phase
B5R: (*E*)-3-(4-((4-(decyloxy)phenylimino)pentyl)benzoyloxy)phenyl 4-((4′-cyanobiphenyl-4-yloxy)methoxy)benzoate.
B6R: (*E*)-3-(4-((4-(decyloxy)phenylimino)hexyl)benzoyloxy)phenyl 4-((4′-cyanobiphenyl-4-yloxy)methoxy)benzoate.
B7R: (*E*)-3-(4-((4-(decyloxy)phenylimino)heptyl)benzoyloxy)phenyl 4-((4′-cyanobiphenyl-4-yloxy)methoxy)benzoate.

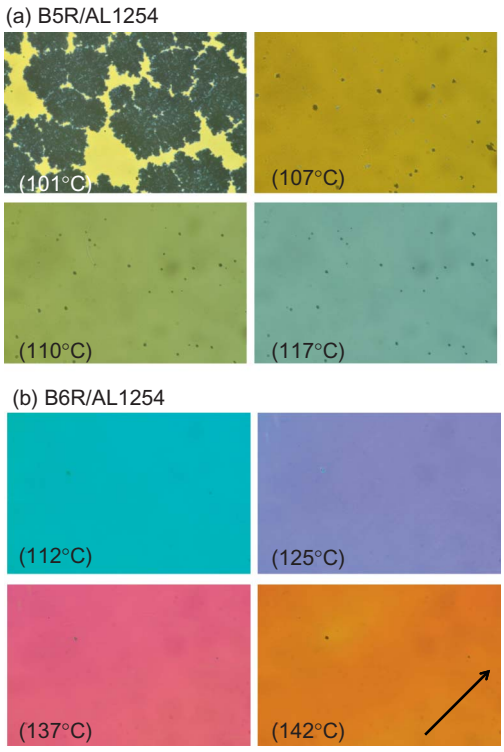

Figure 2. Polarised optical micrographs of (a) B5R and (b) B6R in cells with planar alignment layer surfaces AL1254. In both cells the surfaces were rubbed along the direction shown by the arrow, and good homogeneous alignment was obtained.

3. Results

The normal alignment without an anchoring transition will first be described. Figure 2 shows photomicrographs of (a) B5R and (b) B6R in cells with the planar surface agent, AL1254. The director was uniformly well-aligned along the rubbing direction (arrowed in Figure 2). A completely dark state was observed by rotating the cells. In B5R, the nematic phase emerged from the crystalline phase at 101°C. On heating, the uniform texture colour changes gradually occurred due to a decrease in the birefringence or the orientational order parameter. A similar situation occurred for B6R.

Two differences can be observed in Figure 3:

(1) A larger thermal hysteresis was observed at the nematic–isotropic phase transition in B5R, consistent with the DSC data; and
(2) B6R gave a larger birefringence than B5R.

Since AL1254 is known to provide planar alignment with low pretilt angles of about 2° [7, 8], these birefringences were used as $\Delta n = n_e - n_o$ for the analysis of the director tilt angle with respect to the normal surface, θ, for B5R and B6R on other surfaces. Here n_o and n_e are the ordinary and extraordinary

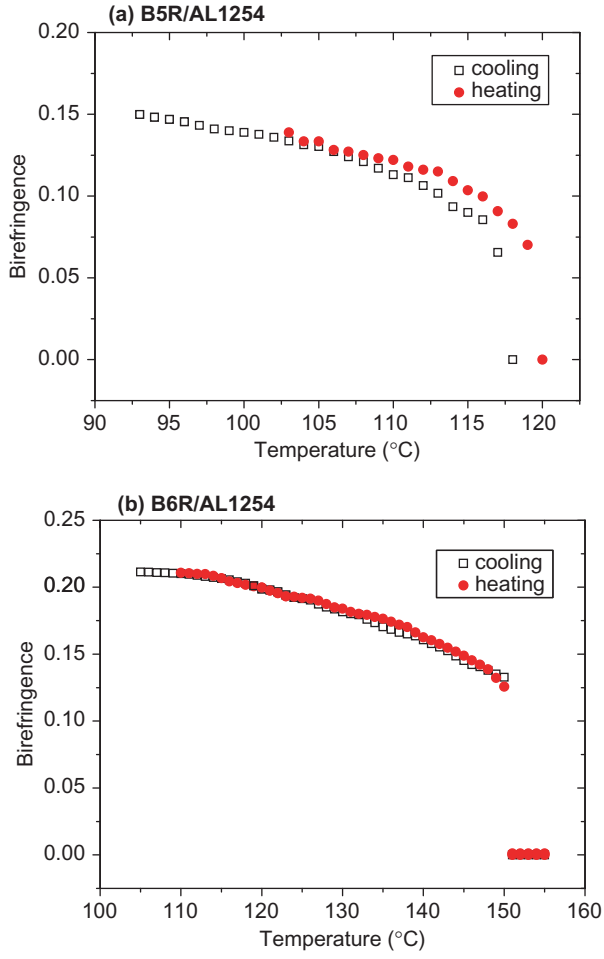

Figure 3. Birefringence of (a) B5R and (b) B6R in cells with planar alignment layer surfaces AL1254 as a function of temperature. Large thermal hysteresis was observed only in B5R, consistent with the DSC measurement (see Table 1).

refractive indices, respectively. By assuming $n_o = 1.5$, it was possible to obtain n_e from Δn in Figure 3. In the following experiment, we obtained $\Delta n_{eff} = n_{eff} - n_o$, and then n_{eff}. By substituting all n_o, n_e, and n_{eff} in the equation

$$n_{eff} = n_e n_o \left(n_o^2 \sin^2\theta + n_e^2 \cos^2\theta\right)^{-1/2}, \qquad (1)$$

θ can be determined.

On homeotropic alignment agent JALS204, B5R was well aligned homeotropically, becoming completely dark under crossed polarisers. In contrast, B6R showed a planar alignment on cooling an unrubbed cell from the isotropic phase. On lowering the temperature slightly dark spots appeared (Figure 4(a), upper left), showing a schlieren texture, and then became completely dark. Thus, B6R showed a first-order anchoring transition from planar to homeotropic on cooling, and *vice versa* on heating.

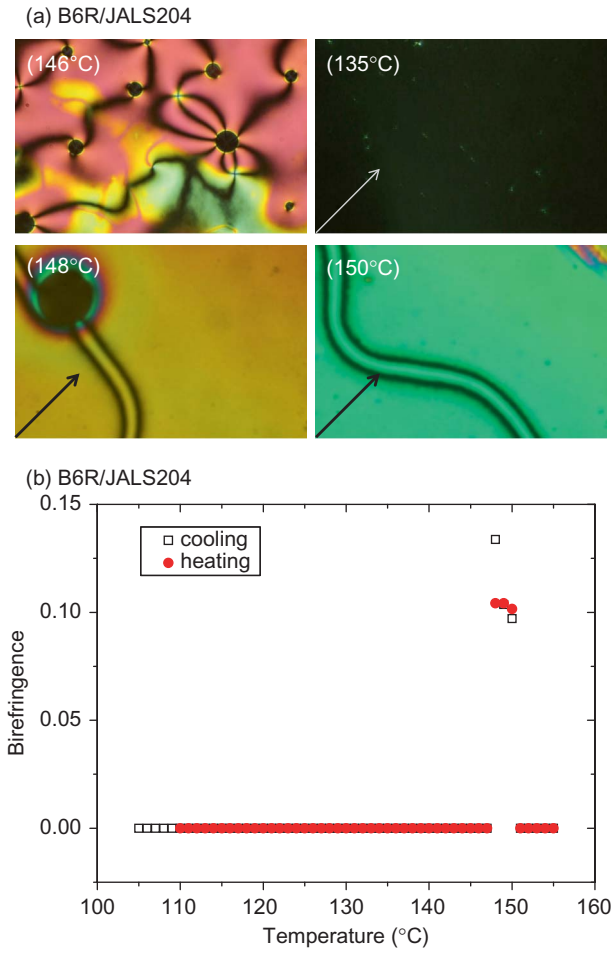

Figure 4. (a) Polarised optical micrographs of B6R in a cell with homeotropic alignment layer surfaces JALS204. The texture at 146°C was obtained using an unrubbed cell. The other three textures were obtained using a rubbed cell (the arrow shows the direction of rubbing) on heating. The first-order anchoring transition from homeotropic (135°C) to homogeneous (150°C) *via* the transition point (148°C) is clearly seen. (b) Birefringence of B6R in cells with homeotropic alignment layer surfaces JALS204 as a function of temperature. Note that B5R did not show any anchoring transition and aligned homeotropically over the whole nematic phase.

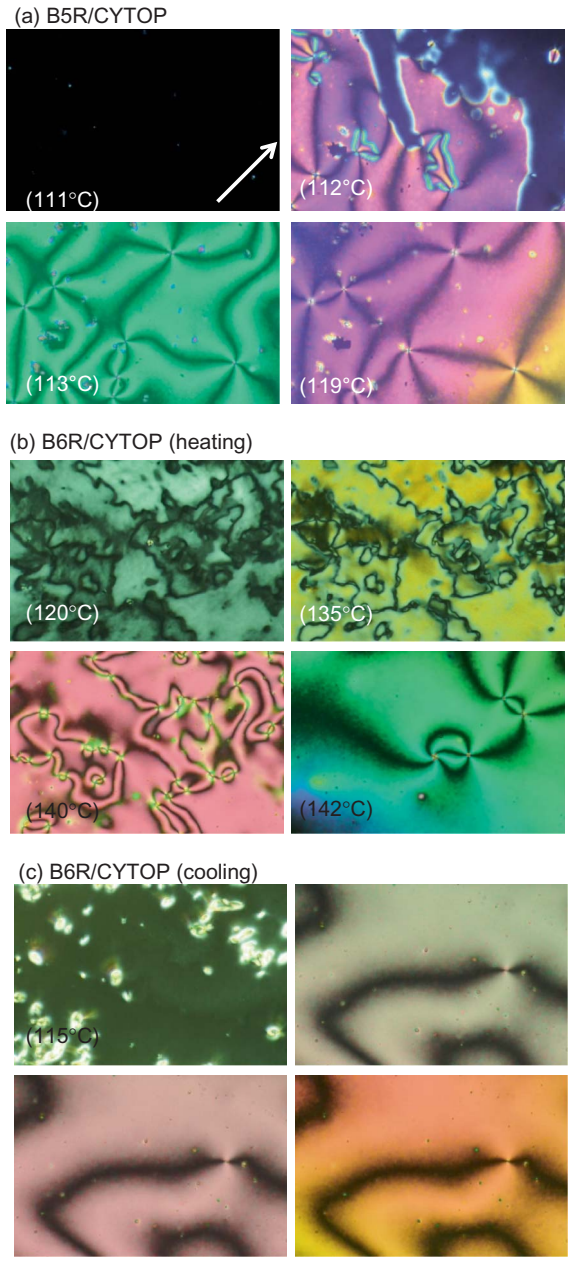

Figure 5. Polarised optical micrographs of (a) B5R in a cell with CYTOP, and (b) and (c) B6R in a cell with CYTOP on heating and cooling, respectively. Both cell surfaces were rubbed in the direction of the arrow. However, the rubbing does not affect the alignment. For B5R, the texture change was abrupt (see the textures at 111°C and 112°C), whereas the changes are gradual for B6R. A difference in behaviour on heating and cooling is also noted; on cooling only a birefringence change was observed, whereas on heating a texture change was associated with the birefringence change.

Texture changes on heating a rubbed cell (arrow direction) are shown in the other photographs in Figure 4(a). The homeotropic alignment remained unchanged down to the SmA phase. According to analysis using Equation (1) and the birefringence data shown in Figure 4(b), the tilt angle was about 45°.

CYTOP also gave a significant difference in anchoring transition behaviour between B5R and B6R. On heating B5R to 111°C its dark homeotropic texture suddenly changed to a colourful texture and the colour changed slightly with further temperature change, as shown in Figure 5(a). In B6R, on the other hand, the texture was not completely darkened even at low temperature, but became progressively brighter with schlieren textures on heating (Figure 5(b)). On cooling, a similar progressive change was observed, as

seen in Figure 5(c). As indicated by the existence of schlieren texture, rubbing was not sufficiently effective to align the director in the direction of rubbing.

Figure 6 reveals the temperature dependence of the birefringence for (a) B5R and (b) B6R. The colour changes in Figure 5(a) indicated a slight birefringence change due to a minor change in the tilt angle from 45° to 48°. Thus, B5R exhibited a first-order anchoring transition on CYTOP surfaces (see Figure 6(a)). In contrast, the birefringence variation in B6R was totally different, as indicated by the texture changes (see Figure 5(b) and 5(c)). On cooling, birefringence increased in the higher temperature range of the nematic phase, then after passing through a maximum birefringence it decreased with further decrease in temperature almost to zero (see Figure 6(b)). It is noted that this very small non-zero birefringence corresponds to a small tilt angle of about 4°. The maximum tilt angle around 135°C was about 47°. On heating, the birefringence change was more or less similar to that on cooling, although a small stepwise change was detected. Different birefringence changes between heating and cooling were also observed for the changes in the texture, i.e., only the colour changed on cooling (Figure 5(c)) without change in texture, whereas both texture and colour changed on heating (Figure 5(b)).

As we have mentioned, it was surprising that two homologues with such a small difference in spacer length, involving only a single carbon atom, exhibited quite different anchoring transition behaviour. In order to understand this phenomenon further, dielectric measurements were conducted on the two homologues. Figure 7 shows the frequency dependence of the real part of the dielectric constant of (a) B5R at 100°C and (b) B6R at 130°C.

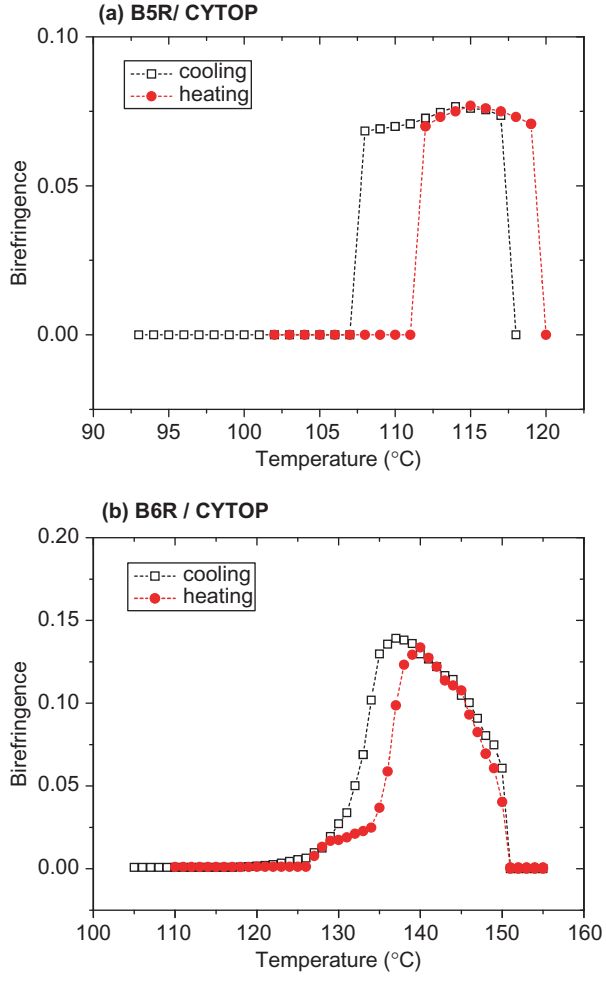

Figure 6. The temperature dependence of the birefringence of (a) B5R and (b) B6R in cells with CYTOP. Sudden and gradual changes were observed with B5R and B6R, respectively.

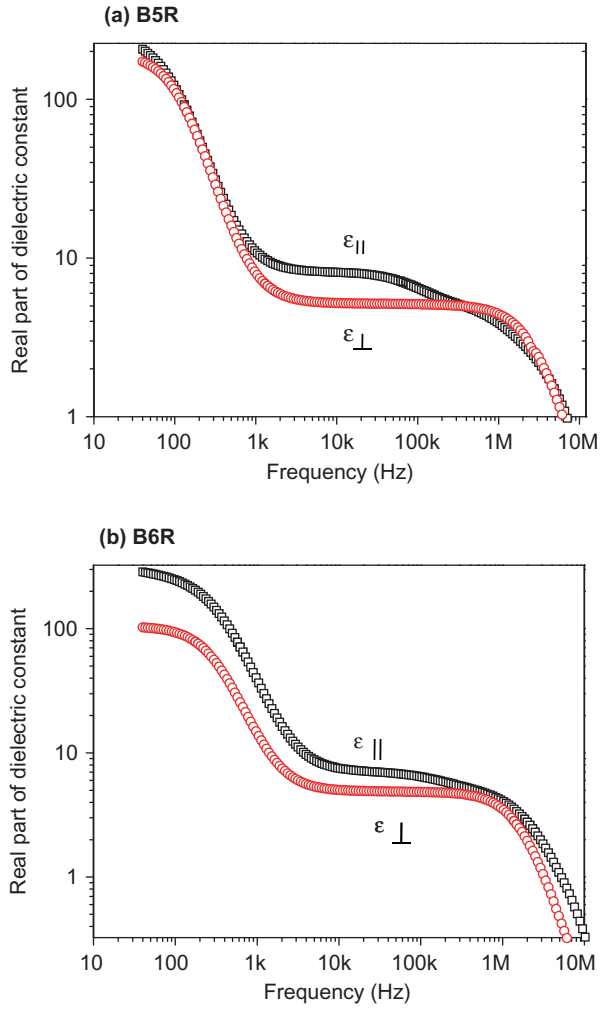

Figure 7. The real part of the dielectric constant of (a) B5R and (b) B6R in the nematic phase.

Measurements were also conducted under a dc-bias field. Suppression of the large dispersion around 100 Hz suggested an ionic contribution. However, the suppression behaviour in planar and homeotropic cells were noticeably different. Considering the relatively high relaxation frequency (~100 Hz) together with the suppression behaviour mentioned previously, an assignment to an ionic contribution is not straightforward. The details will be reported in a separate paper.

Certain experimental features are observed in Figure 7:

(1) the dielectric anisotropy is positive for both B5R and B6R;
(2) the anisotropy is larger for B5R than B6R around 10 kHz but is larger for B6R than B5R around 100 Hz;
(3) the relaxation frequency for B5R is lower (~200 Hz) than that for B6R (~600 Hz); and
(4) there is additional relaxation at around 200 kHz for the parallel component, particularly for B5R, whereas the perpendicular component showed only a simple relaxation due to ITO at about 3 MHz.

The bent-core mesogen has a transverse average dipole, whereas the cyanobiphenyl mesogen has a longitudinal average dipole. The relative directions of these dipoles are affected by the number of carbons in the spacer n, so that electric properties such as the dielectric anisotropy are influenced by the spacer length n. As shown in Figure 8 for an all-trans conformation, the transverse component of the CN group is parallel and antiparallel to the bend direction of the bent-core mesogen in B5R and B6R, respectively, although the longitudinal components for B5R and B6R should have a smaller dependence on n. The conformational difference may account for the difference in the dielectric behaviour, and in turn the different anchoring transition behaviour, between B5R and B6R.

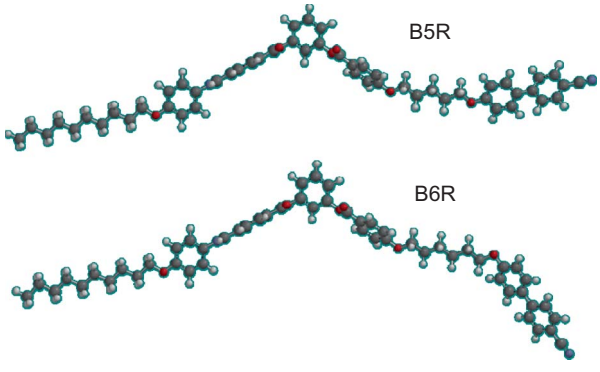

Figure 8. Molecular structures of B5R and B6R in their extended conformations. Note the relative orientations of the rod-shaped mesogens with respect to a bent-shaped mesogen.

4. Discussion

A similar bend-rod liquid crystal dimer has been synthesised by Yelamaggad *et al.* [13], who suggested the existence of a biaxial nematic and a smectic A phase. As we mentioned earlier in the Introduction, Prasad *et al.* have reported a N_B–N_U phase transition [4], although the existence of a N_B phase was later challenged [3]. Hence, a transition between N_B and N_U might have been proposed, even in the present case. However, a uniaxial-like non-birefringent phase emerged below the birefringent phase. If we assign this change to the N_U–N_B phase, N_U would be a lower temperature phase than N_B. This is not possible, however, so the birefringence change may definitely be ascribed to an anchoring transition.

To describe the anchoring transition caused by temperature changes, we have to consider that the interactions with surfaces are affected by the nematic orientational order. We only consider the van der Waals interactions with surfaces, which strongly depend on distance. If the molecular interactions with the surfaces are of a similar strength to those between the molecules themselves, it is possible that with increasing nematic order the orientation with respect to the surface changes significantly. For relatively disordered molecules their arrangement with respect to the surface can be very different than for molecules which are well ordered.

The anchoring interaction can be described within a Landau-like theory [14] by

$$f_{\text{surface}} = \frac{1}{2}(\beta_1 S - \beta_2 S^2)(\mathbf{n}\cdot\ \mathbf{k})^2 + \frac{1}{4}\beta_3 S^2(\mathbf{n}\cdot\mathbf{k})^4 + \frac{1}{6}\beta_4 S^3(\mathbf{n}\cdot\ \mathbf{k})^6 \qquad (2)$$

where S is the nematic order parameter for the liquid crystal in a cell, $\mathbf{n}$ is a director, $\mathbf{k}$ is a surface normal, and β_1, β_2, β_3 and β_4 are coefficients which give the anchoring interaction energy. As mentioned by Nazarenko and Lavrentovich [14], the quadratic term in the contribution to the free energy can indicate various orientations of the nematic in the cell. The orientation of the nematic is expressed by$(\mathbf{n}\cdot\mathbf{k}) = \cos\theta \equiv T$, where θ gives the tilt angle with respect to the surface normal. The sixth-order term is included for the sake of completeness, as the anchoring contribution now allows for discontinuous orientational transitions as well. It is also reasonable to expect higher order terms, as the van der Waals interactions are highly non-linear.

It has been assumed in the present study that the anchoring does not significantly influence the magnitude of the nematic order, but that the opposite is true; that is, changing the orientational order influences the strength of the anchoring. As the interactions with the surfaces and between molecules are of the van der Waals type, it is reasonable to expect that higher order terms for the ordering have to be included.

Minimisation of free energy with respect to the surface orientation $T = \cos\theta$ gives

$$(\beta_1 S - \beta_2 S^2)T + \beta_3 S^2 T^3 + \beta_4 S^3 T^5 = 0 \qquad (3)$$

with three different possible solutions, including

$$T = 0. \qquad (4)$$

The solution is stable for positive values of $(\beta_1 S - \beta_2 S^2)$ and this means that the surface order is tangential. Within this consideration the preferred direction is arbitrary so long as it is perpendicular to the surface normal. In practice, however, the degeneracy is lifted by surface treatment such as rubbing, and so an easy axis results.

For qualitative reasoning let us neglect the sixth-order term for the moment. Then the stable solution is obtained:

$$T^2 = -\frac{\beta_1 S - \beta_2 S^2}{\beta_3 S^2}, \qquad (5)$$

which is stable for negative values of $(\beta_1 S - \beta_2 S^2)$ and actually presents two different structures. If $|(\beta_1 S - \beta_2 S^2)| > \beta_3 S^2$, the solution gives the perpendicular orientation of the director with respect to the surface normal with T=1, i.e. homeotropic alignment, with $\theta = 0$. If on the other hand $|(\beta_1 S - \beta_2 S^2)| < \beta_3 S^2$, $0 < T < 1$; i.e. the structure is tilted in a general direction with respect to the surface normal and $0 < T < 1$, and the tilt angle θ has a general value. Additional sixth-order terms in T make the expression in Equation (5) more complicated, but qualitatively they may change only the order of the transition between the tilted homeotropic and planar orientations, as well as being able to expel the tilted structure.

Let us now consider the experimental observations within the framework of our model. All of the parameters, β_i, originate mainly from van der Waals interactions and are obviously different for different molecules and different surfaces. The interactions with surfaces in AL1254 cells were used as a reference. We can say that over the whole range of nematic order for both materials, $(\beta_1 S - \beta_2 S^2) > 0$, which gives the tangential planar ordering. However, in the JALS204, which in liquid crystalline materials usually induces homeotropic alignment, B6R exhibited an anchoring type transition. Various types of interaction with surfaces seem to be competing in this material and they change with increasing nematic order, S. The temperature dependence of S is approximated by $S = [1 - (T/T_0)]^{\gamma}$. Bearing in mind that the transition is first order, γ became approximated to ¼, and using the transition temperature T_0 in Figure 3(a) and (b), the temperature dependence of S shown in Figure 9(a) and (b) was obtained for B5R and B6R, respectively.

As seen in Figure 4, homeotropic alignment is not achieved in the JALS204 cell for B6R, when the nematic phase becomes stable on cooling. On lowering the temperature and with the consequent increasing nematic order the system changes discontinuously to homeotropic alignment. The system minimises the free energy due to the competing interactions by adopting the general tilt angle with respect to the normal layer, as is seen in Figure 10(a). The free energy minimum close to the N–I transition is rather shallow (Figure 10(b)), which means that fluctuations and defects can induce the discontinuous transition to the homeotropic state. Thus, the minimisation of the free energy in Equation (2)

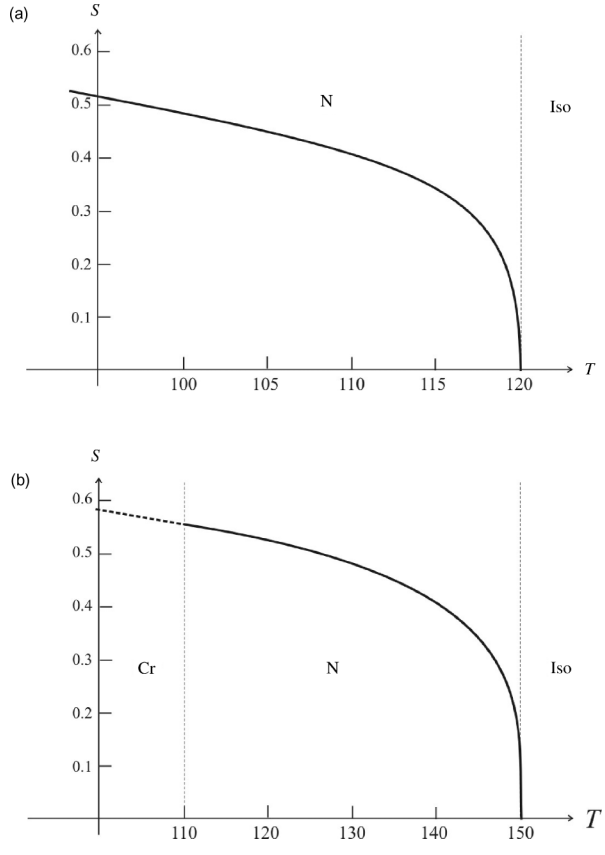

Figure 9. The calculated temperature dependence of the nematic order parameter S for (a) B5R and (b) B6R.

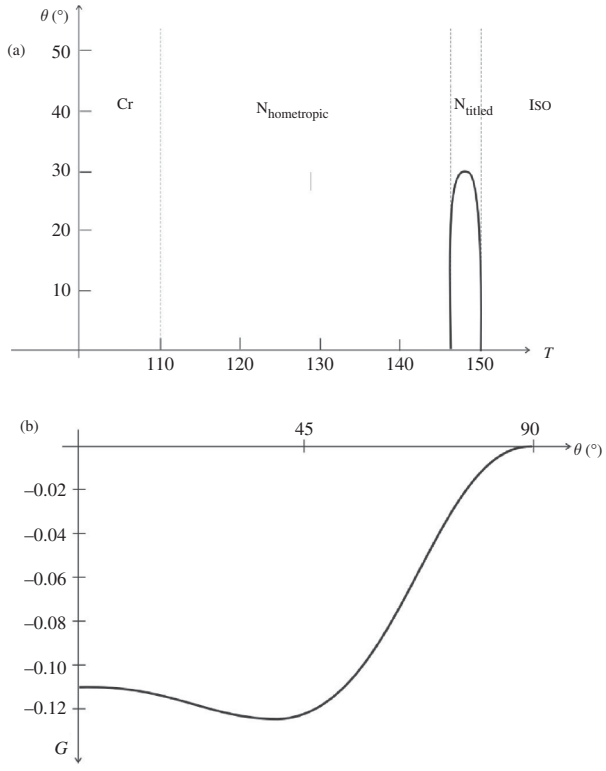

Figure 10. (a) The calculated temperature dependence of the director tilt with respect to the surface normal for B6R in the JALS204 cell. Model coefficients used for the calculations are: $\beta_1 = -1$; $\beta_2 = -4$; $\beta_3 = 10$; $\beta_4 = -18$. (b) The free energy of the surface interactions close to the transition temperature at $S = 0.47$ shows a relatively shallow minimum for the tilted solutions. The units of free energy are arbitrary.

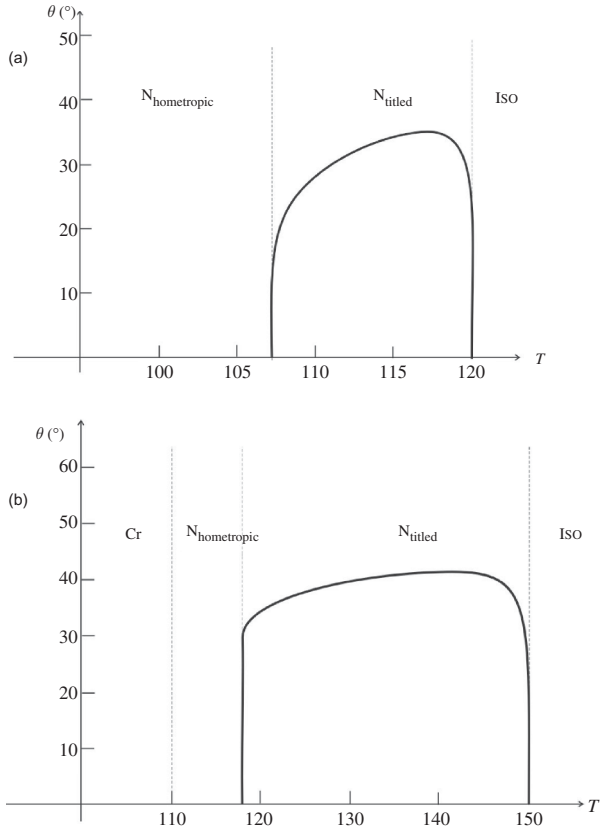

Figure 11. The calculated temperature dependence of the director tilt with respect to the surface normal for (a) B5R and (b) B6R in the CYTOP cell. The lack of dependence of the tilt on temperature is clearly seen in both cases. The coefficients used for the calculations were (a) $\beta_1 = -1$; $\beta_2 = -5.8$; $\beta_3 = 10$; $\beta_4 = -12.2$ and (b) $\beta_1 = -1.3$; $\beta_2 = -4$; $\beta_3 = 12$; $\beta_4 = -15$.

can, qualitatively, reproduce well the observed behaviour (compare Figure 4(b) and Figure 10(a)).

Finally, with a slight change in the model coefficients we can also reproduce the behaviour of both materials when introduced into the CYTOP cells. From Figure 6 one can see evidence of re-entrant behaviour; the tilt first increases and then decreases upon lowering the temperature. Although the different behaviour of the first- and second-order anchoring transitions in B5R and B6R cannot be reproduced, qualitative reproduction of their behaviour is made in Figures 11(a) and 11(b) for B5R and B6R, respectively.

Conclusions

Anchoring transitions due to changing temperature were observed for two homologous compounds consisting of bent- and rod-shaped mesogens linked by a polymethylene spacer. The transitional behaviour depended on the liquid crystal materials and the surfaces involved. With a homeotropic surface active agent, one compound simply exhibited homeotropic alignment, whereas the other compound showed a tilted structure immediately after cooling from the isotropic phase and then changed its orientation to homeotropic alignment. On a perfluoropolymer surface, these compounds showed first- and second-order anchoring transitions. Qualitative description of the anchoring transition behaviour was successfully made using a phenomenological theory.

References

[1] Yu, L.J.; Saupe, A. *Phys. Rev. Lett.* **1980**, *45*, 1000–1003.
[2] Boonbrahm, P.; Saupe, A. *J. Chem. Phys.* **1984**, *81*, 2076–2081.
[3] Le, K.V.; Mathews, M.; Chambers, M.; Harden, J.; Li, Q.; Takezoe, H.; Jalki, A. *Phys. Rev. E: Stat., Nonlinear, Soft Matter Phys.* **2009**, *79*, 030701(R)–1–4.

[4] Prasad, V.; Kang, S.-W.; Suresh, K.A.; Joshi, L.; Wang, Q.; Kumar, S. *J. Am. Chem. Soc*. **2005**, *127*, 17224–17227.
[5] Dhara, S.; Kim, J.K.; Jeong, S.M.; Kogo, R.; Araoka, F.; Ishikawa, K.; Takezoe, H. *Phys. Rev. E: Stat., Nonlinear, Soft Matter Phys.* **2009**, *79*, 060701(R)–1–4.
[6] Aoki, Y.; Watabe, T.; Hirose, T.; Ishikawa, K. *Chem. Lett*. **2007**, *36*, 380–381.
[7] Faget, L.; Lamarque-Forget, S.; Martinot-Lagarde, P.; Auroy, P.; Dozov, I. *Phys. Rev. E: Stat., Nonlinear, Soft Matter Phys.* **2006**, *74*, 050701(R)–1–4.
[8] Patel, J.S.; Yokoyama, H. *Nature* **1993**, *362*, 525–527.
[9] Jerome, B. *Rep. Prog. Phys*. **1991**, *54*, 391–451.
[10] Kimura, H. *J. Phys. Soc. Jpn*. **1993**, *62*, 2725–2733.
[11] Wang, B.; Yamaguchi, R.; Ye, M.; Sato, S. *Jpn. J. Appl. Phys*. **2002**, *41*, 5307–5310.
[12] Kikuchi, H.; Yamamoto, H.; Sato, H.; Kawakita, M.; Takizawa, K.; Fujikake, H. *Jpn. J. Appl. Phys*. **2005**, *44*, 981–989.
[13] Yelamaggad, C.V.; Prasad, S.K.; Nair, G.G.; Shashikala, I.S.; Shankar Rao, D.S.; Lobo, C.V.; Chandrasekhar, S. *Angew. Chem., Int. Ed.* **2004**, *43*, 3429–3432.
[14] Nazarenko, V.G.; Lavrentovich, O.D. *Phys. Rev. E: Stat., Nonlinear, Soft Matter Phys.* **1994**, *49*, 990(R)–993(R).